journal

J. Am. Ceram. Soc., 83 [6] 1428–32 (2000)

Scratch Damage in Zirconia Ceramics

Seung Kun Lee,*,† Rajan Tandon,* and Michael J. Readey*

Caterpillar, Inc., Peoria, Illinois 61656

Brian R. Lawn*

Material Science and Engineering Laboratory, National Institute of Standards and Technology, Gaithersburg, Maryland 20899

Scratch damage modes in zirconia-based ceramics—Mg-PSZ, Y-TZP, and Ce-TZP—are investigated. Precursor indentation tests with a tungsten carbide sphere foreshadow the nature of damage: in Mg-PSZ, extensive (quasi-)plastic deformation in the region outside and beneath the contact; in Y-TZP, less plastic deformation beneath the contact but incipient cone cracking in the region of tension outside the contact; in Ce-TZP, intermediate behavior. Scratch testing is conducted using a conical diamond indenter. In all materials the damage mode changes from smooth plastic deformation to limited cracking with increasing scratch load: in Mg-PSZ, plastic deformation is predominant at lower loads, with microcracking at higher loads; in Y-TZP, plastic deformation is predominant over the range of the test loads—macrocracks initiate only at relatively high loads, but penetrate to a relatively large depth; again, Ce-TZP shows intermediate behavior, but with cracking patterns closer to that of Mg-PSZ. Bending tests on specimens subjected to scratch damage indicate a relatively high damage tolerance in the Mg-PSZ and Ce-TZP; Y-TZP shows the highest initial strength, but suffers relatively large strength loss above the critical load for macrocracking. Implications concerning relative merits of each zirconia type for wear properties, contact fatigue, and machining damage are briefly discussed.

I. Introduction

ZIRCONIA-BASED ceramics with high wear resistance have been identified as choices for sliding components in a variety of engineering applications, including engine components (bearings, rollers, dies, tappets, valves, fuel injectors) and biomechanical components (dental restorations, hip prostheses), where contact, scratch, and wear damage are critical factors for lifetime performance.[1–4] Energy absorptive phase transformation from metastable tetragonal phase to monoclinic phase enhances fracture toughness in this class of ceramics.[5–9] Much progress has been made during the past 25 years in this kind of toughness enhancement in zirconias, by microstructural control through modification of selective additive phases (MgO, Y_2O_3, CeO) and heat treatments.[10–13] Properties like fatigue[14] and machining and wear[15,16] have been demonstrated to be strongly affected by such microstructural factors.

Hertzian testing using spherical indenters is providing new insights into the role of microstructure in such properties. In Mg-PSZ, the mode of contact damage changes dramatically with the degree of heat-treatment aging, from distributed microcracking (underaged) to phase transformation (peak-aged), back to microcracking (overaged).[14] In Y-TZP, the mode is mainly phase transformation.[17] Scratch testing using a translating sharp point provides more direct information on potential processes in wear and machining operations.[15,16,18] Data from these two test procedures may be expected to provide complementary basic information on damage modes in engineering contact and sliding applications, as well as on material removal in wear and machining and flaw development in strength determination.

In this study we investigate contact and scratch damage in selected Mg-PSZ (peak-aged), Y-TZP, and Ce-TZP materials. The results demonstrate a need for caution in materials selection for applications in severe contact conditions.

II. Experimental Procedure

Three commercially available zirconias, with Mg-, Y-, and Ce-stabilizing additives, were chosen for this study. Table I summarizes basic material properties as measured by conventional means. Surfaces were diamond polished to 1 μm finish for indentation and scratch testing.

Indentations were made on each material using tungsten carbide (WC) spheres of radius $r = 3.18$ mm, at peak loads up to $P = 3000$ N, in air (relative humidity 45%–55%).[19]

Scratches were made using a sliding conical diamond indenter with apex angle 120° and spherical tip radius 200 μm (Automatic Scratch Tester, CSEM-REVETEST, Neuchatel, Switzerland). In automatic test mode, the load is increased continuously as the point translates across the surface. Both normal and tangential forces were recorded. Normal loads ranged from $P = 5$ N to 130 N over about 20 mm sliding distance, at sliding speed 20 mm·min^{-1}, in air. A piezoelectric accelerometer was used to record the intensity of acoustic signals. Cross-sectional areas of the scratches were measured with a surface profilometer, to obtain an estimate of the volume removed per unit sliding distance. Some additional scratch tests were made on selected specimens, at prescribed constant loads (see below).

Bonded-interface specimens[14,16,19,20] were used to obtain section views through the indentation and scratch damage zones in each material. Specimens were cut into two half-blocks. The side surfaces of the half-blocks were first polished and then clamped face-to-face with an intervening thin layer of adhesive. The top surfaces were then repolished. Indentations were made along the surface traces of the bonded interfaces, at load $P = 3000$ N. Scratch tests were made perpendicular to these interfaces, at load $P = 100$ N. The adhesive joining the interfaces was subsequently dissolved in acetone. Separated half-blocks were gold coated for top- and side-surface examination in Nomarski illumination. The validity of the bonded-interface technique in its capacity to reveal the true nature of the contact damage has been documented.[14,16]

Four-point bending tests were conducted on bars 3 mm × 4 mm × 45 mm (outer span 40 mm, inner span 20 mm) that had been

R. O. Scattergood—contributing editor

Manuscript No. 189278. Received June 18, 1999; approved December 8, 1999.
*Member, American Ceramic Society.
†Contracted under Adecco TAD Technical, Peoria, Illinois 61615.

Table I. Material Characteristics

Material	Phase (%)[†] Polished surface	Grain size (μm)	Toughness[‡] (MPa·m$^{1/2}$)	Strength[§] (MPa)	Hardness[¶] (GPa)
9 mol% Mg-PSZ[††]	Monoclinic (13) Tetragonal (33) Cubic (54)	58	12.5 ± 0.5	585 ± 34	10.0
3 mol% Y-TZP[‡‡]	Tetragonal (100) Monoclinic (0)	0.4	5.3 ± 0.9	986 ± 91	13.6
12 mol% Ce-TZP[§§]	Tetragonal (100) Monoclinic (0)	2.5	8.9 ± 0.3	514 ± 20	9.9

[†]Determined by X-ray analysis. [‡]Indentation method[18] (P = 196 N). [§]Four-point bending strength. [¶]Indenter load = 196 N. [††]Carpenter Inc., TS grade. [‡‡]Kennametal Inc., Z55 grade. [§§]Ferro Corp., Zirmonite 1000.

subjected to scratch damage. The scratches were made on the prospective tensile surfaces, with the scratch axis parallel to the prospective bend axis, at loads P = 20 to 130 N. The damage areas were covered with a drop of dry silicon oil before flexure and broken in fast fracture (<10 ms), to minimize environmental effects in the strength data. All broken specimens were examined fractographically to locate the source of failure, either scratch damage or extraneous flaws. Control strength tests were made on unscratched specimens, to determine baseline laboratory strengths.

III. Results

Figure 1 shows half-surface and side views of contact damage for each material, at common load P = 3000 N. All materials show a residual depression at the contact center on the top surface. There are faint traces of incipient ring cracks in each material. Subsurface damage depends strongly on the material, with surface rumpling characteristic of phase transformations.[8,14] The deformation zone is most intense in the Mg-PSZ, least in the Y-TZP. Some microcracking is observed beneath the contact in the Mg-PSZ, where shear stresses are a maximum, similar to that in coarse-grain alumina.[21] Similar microcracking damage, albeit on a reduced scale, is seen in the Ce-TZP. No such microcracking is evident in the Y-TZP; in this latter case an incipient cone crack has begun to form.

Figure 2 shows the variation of acoustic emission and tangential frictional force with normal scratch load for Mg-PSZ, Y-TZP, and Ce-TZP. Corresponding scratch damage patterns are included in the upper portion of each figure. Consider these results for each material in turn:

(a) Mg-PSZ (Fig. 2(a)). Below normal load (35 N) the scratch groove is smooth, without detectable fracture, indicative of a plastic process. No acoustic signal is registered in this region. Above 35 N limited surface microcracking becomes evident around the scratch groove. An acoustic signal is now detected, and this signal increases in intensity with progressing translation. Above 75 N the cracking becomes extensive, with some chipping. The acoustic intensity correspondingly accelerates, and the frictional force begins to increase and fluctuate.

(b) Y-TZP (Fig. 2(b)). The damage appears to be fully plastic along the entire scratch groove. The frictional force increases monotonically with load, corresponding to an approximately constant friction coefficient. Beyond load 100 N the acoustic emission shows an abrupt rise in activity, suggesting some subsurface process.

(c) Ce-TZP (Fig. 2(c)). The scratch shows limited microcracking on the surface, similar to that for Mg-PSZ, but not as intense and not until 70 N (cf. 35 N in Fig. 2(a)). The frictional force increases linearly up to this load, after which it begins to rise more quickly and to fluctuate slightly. The acoustic intensity begins to rise above the critical load, at a rate somewhere between those of the other zirconias.

Figure 3 shows surface and side views of scratch damage of the three materials from bonded-interface specimens at P = 100 N, i.e., in the high-load region of Fig. 2. In Mg-PSZ (Fig. 3(a)) a diffuse microcrack zone extends well below the surface groove into the subsurface. In the near-surface regions, these microcracks have coalesced to produce extensive chipping. In Y-TZP (Fig. 3(b)) no microcracking is observed at all; instead, a deeply penetrating median crack is evident immediately below the smooth

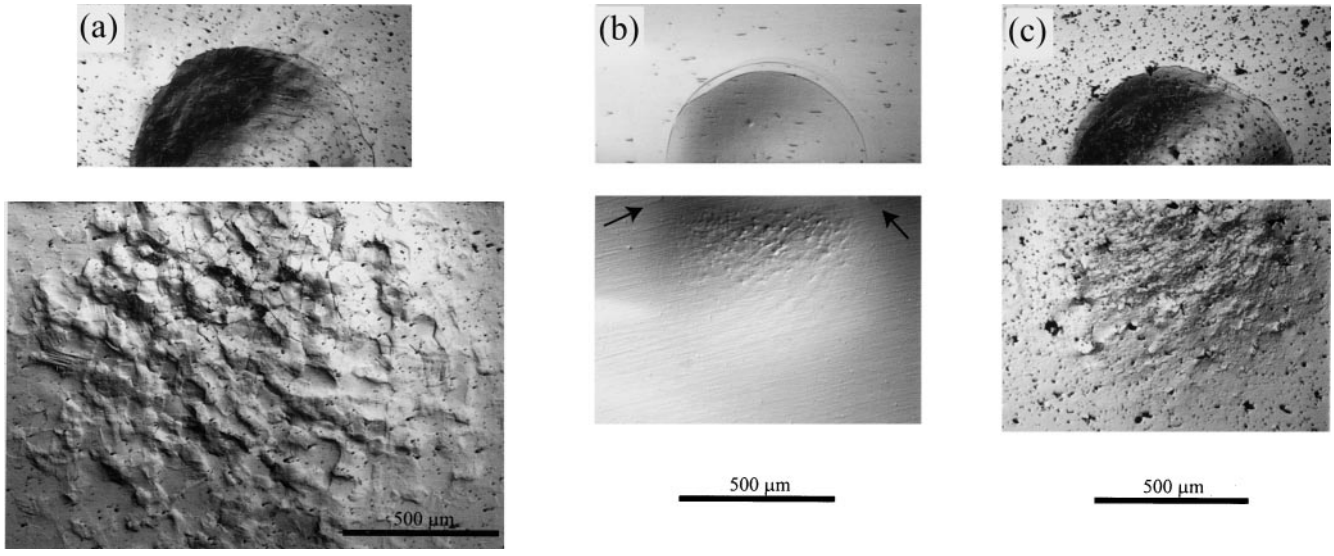

Fig. 1. Half-surface and side views of contact damage in (a) Mg-PSZ, (b) Y-TZP, and (c) Ce-TZP, from WC sphere radius r = 1.98 mm at load P = 3000 N. Nomarski optical micrographs of bonded-interface specimens.

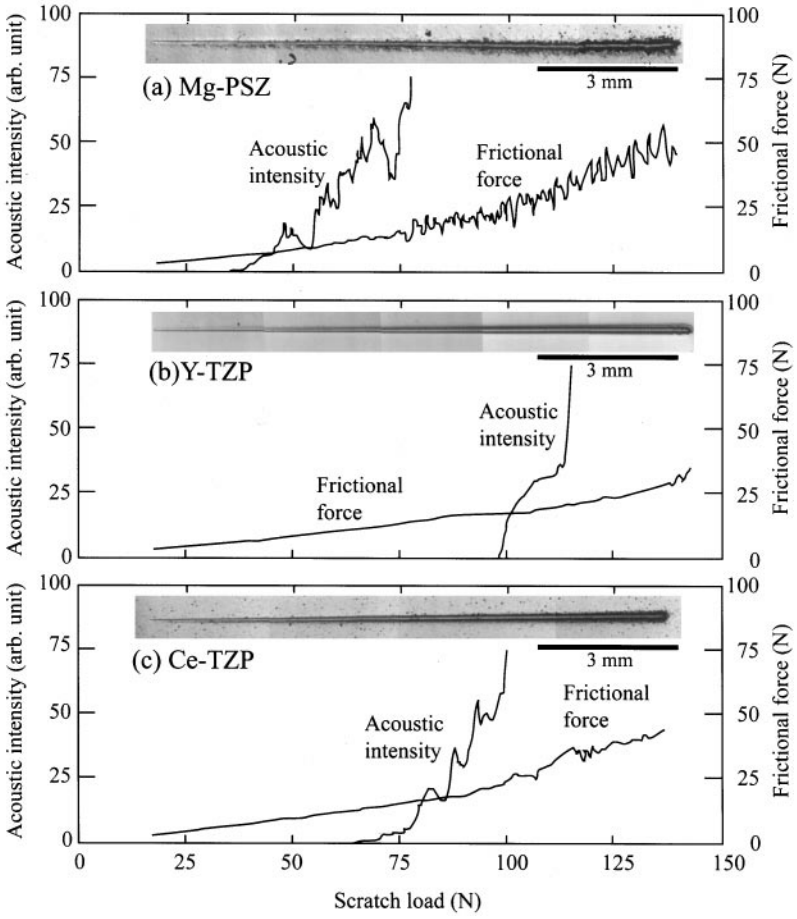

Fig. 2. Acoustic signal intensity and frictional force, as function of increasing scratch load, for (a) Mg-PSZ, (b) Y-TZP, and (c) Ce-TZP Mg-PSZ. Surface views of scratches included.

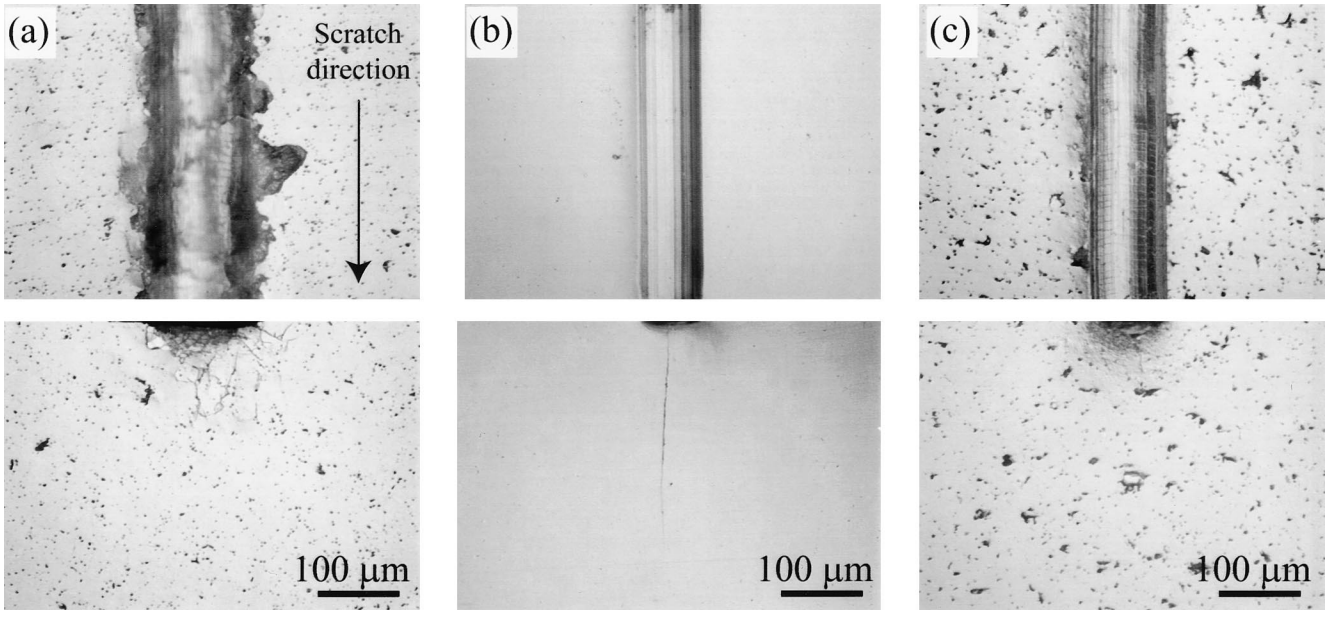

Fig. 3. Top and side views of scratch damage of Mg-PSZ, Y-TZP, and Ce-TZP, scratch load $P = 100$ N.

scratch. In Ce-TZP (Fig. 3(c)) limited microcracking is observed, on a smaller scale than in Mg-PSZ.

Figure 4(a) is a plot of volume removed per unit sliding distance as a function of normal load for the three materials, evaluated from surface profilometer traces across the scratches. Mg-PSZ ultimately shows the most severe wear rate, above load 75 N where surface microcracking and chipping are manifest. Y-TZP shows the lowest removal rate, over the entire range of loads.

Figure 4(b) compares strength degradation data for scratch damage on the three materials. In the Mg-PSZ and Ce-TZP, strength falls off beyond the load for extensive microcracking, but only slowly, indicating high damage tolerance. Y-TZP, on the

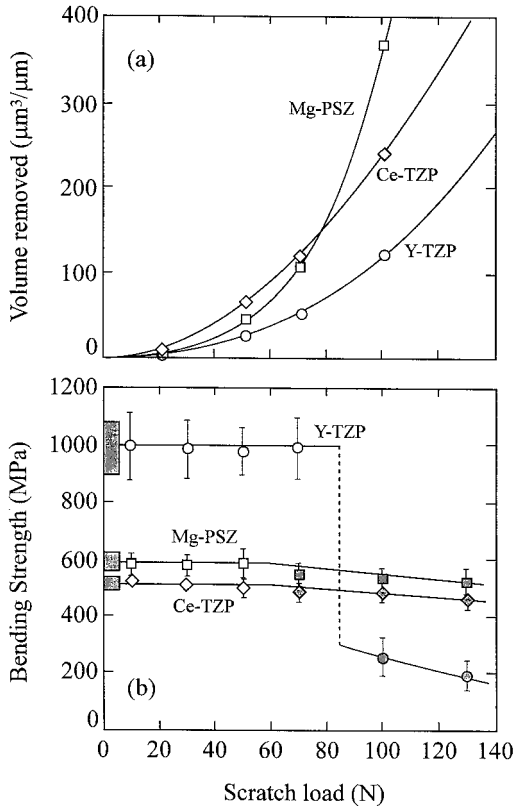

Fig. 4. Wear and strength properties in scratching of Mg-PSZ, Y-TZP, and Ce-TZP, as a function of load: (a) volume removed along scratch length; (b) ensuing bending strength. Data points are means and standard deviations for a minimum of five specimens. Closed symbols represent failures from scratch origins, open symbols failures from other flaw origins. Solid lines are empirical fits; shaded boxes at left are strengths of as-polished specimens.

other hand, shows a typical brittle response; i.e., no perceptible degradation in initially high strength up to about 80 N, but with subsequent abrupt drop-off at higher loads, highlighting the effectiveness of the median crack in Fig. 3(c).

IV. Discussion

We have investigated contact and scratch damage in three commonly available zirconias—Mg-PSZ, Y-TZP, and Ce-TZP. From the contact damage patterns in Fig. 1, it is readily apparent that the Mg-PSZ is the most transformable of the three, Y-TZP the least, and Ce-TZP intermediate. This correlates directly with the hardness, and inversely with the toughness, in Table I. Mg-PSZ is characterized by limited diffuse subsurface microcracking, Y-TZP by more well-defined surface ring cracks (although its depth is markedly smaller than comparable cone cracks in other brittle materials, like fine-grain aluminas[21] or silicon nitrides[22]), and Ce-TZP again intermediate.

This trend foreshadows the scratch resistance behavior in the three materials. All materials exhibit a plastic–brittle transition with increasing normal load (Figs. 2 and 3). Mg-PSZ shows the least smooth scratch track, with extensive microcracking and associated chipping above a critical load, resulting in a high wear rate at higher loads. Y-TZP shows the smoothest track, and lowest wear rate. Ce-TZP is again intermediate, with modest microcracking. Y-TZP is the most brittle of the three materials, as reflected by the formation of a deeply penetrating median crack in the subsurface region above a critical load. Accordingly, Y-TZP is much more susceptible to abrupt strength loss in severe scratching conditions; its strength drops from almost twice to less than one-half that of its counterparts over the data range. Mg-PSZ and Ce-TZP, on the other hand, while still subject to failure from scratch sites above a threshold load, are much more damage tolerant.

These results emphasize the need for characterization of properties over a wide data range. Y-TZP is likely to perform more creditably where high wear resistance is an issue. In this material, the relatively modest level of phase-transformation-induced toughening (reflected in the toughness values in Table I) appears sufficiently low as to preclude the generation of attendant microcracks. Y-TZP also has high strength, but can lose this strength catastrophically if the contact conditions become severe enough to initiate penetrating macrocracks. Mg-TZP and Ce-TZP retain strength over a wider range of scratch loads,[23] but are prone to exhibit inferior wear[24,25] and fatigue properties,[17,26] where microcrack coalescence can be an especially deleterious mechanism.

V. Conclusions

Hertzian contact damage has been shown to be different in three zirconia materials: Mg-PSZ showed extensive plasticity below the indentation, along with limited surface microcracking; Y-TZP showed much less plasticity, with the onset of deep cone cracks above a critical load; Ce-TZP showed intermediate behavior. Similar trends were observed in the scratch tests: in Mg-PSZ, plastic deformation and extensive distributed surface and subsurface microcracking; in Y-TZP, a smooth scratch track with limited plasticity and, above a critical load, deep cracks; in Ce-TZP, similar to Mg-PSZ, but less pronounced microcracking. In strength tests on surface-scratched specimens, Mg-PSZ and Ce-TZP showed gradual strength degradation with increasing load; but Y-TZP, while initially stronger than its two counterparts, showed an abrupt and substantial strength drop-off beyond the crack initiation load.

References

[1]R. H. J. Hannink, M. J. Murray, H. G. Scott, "Friction and Wear of Partially Stabilized Zirconia: Basic Science and Practical Applications," *Wear*, **100**, 355–66 (1984).

[2]G. W. Stachowiak and G. B. Stachowiak, "Unlubricated Friction and Wear Behavior of Toughened Zirconia Ceramics," *Wear*, **132**, 151–71 (1989).

[3]A. Gangopadhyay, H. S. Cheng, J. F. Braza, S. Harman, and J. Corwin; pp. 329–56 in *Fiction and Wear of Ceramics*. Edited by Said Jahanmir. Marcel Dekker, New York, 1994.

[4]Y. M. Chen, B. Rigaut, and F. Armanet, "Wear Behavior of Partially Stabilized Zirconia at High Sliding Speed," *J. Eur. Ceram. Soc.*, **6**, 383–90 (1990).

[5]R. M. McMeeking and A. G. Evans, "Mechanics of Transformation Toughening in Brittle Materials," *J. Am. Ceram. Soc.*, **65**, 242 (1982).

[6]P. F. Becher, G. Begun, and E. Funkenbusch; pp. 645–51 in Advances in Ceramics, Vol. 24B, *Science and Technology of Zirconia III*. Edited by S. Somiya, N. Yamamoto, and H. Yanagida. American Ceramic Society, Westerville, OH, 1988.

[7]A. G. Evans, "Perspective on the Development of High-Toughness Ceramics," *J. Am. Ceram. Soc.*, **73** [2] 187–206 (1990).

[8]D. B. Marshall, "Reversible Stress-Induced Martensitic Transformation in ZrO_2," *J. Am. Ceram. Soc.*, **69** [3] 215–17 (1986).

[9]D. J. Green, R. H. J. Hannink, and M. Swain, *Transformation Toughening of Ceramics*. CRC Press, Boca Raton, FL, 1989.

[10]R. C. Garvie, R. H. J. Hannink, and R. T. Pascoe, "Ceramic Steel?," *Nature (London)*, **258**, 703 (1975).

[11]A. H. Heuer and L. W. Hobbs (Eds.), Advances in Ceramics, Vol. 3, *Science and Technology of Zirconia*. American Ceramic Society, Columbus, OH, 1981.

[12]N. Claussen, M. Ruhle, and A. H. Heuer (Eds.), Advances in Ceramics, Vol. 12, *Science and Technology of Zirconia II*. American Ceramic Society, Columbus, OH, 1985.

[13] S. Somiya, N. Yamamoto, and H. Yanagida (Eds.), Advances in Ceramics, Vol. 24, *Science and Technology of Zirconia III*. American Ceramic Society, Westerville, OH, 1988.

[14]A. Pajares, F. Guiberteau, B. R. Lawn, and S. Lathabai, "Hertzian Contact Damage in Magnesia-Partially-Stabilized Zirconia," *J. Am. Ceram. Soc.*, **78** [4] 1083–86 (1995).

[15]M. V. Swain, "Microfracture About Scratches in Brittle Solids," *Proc. R. Soc. London*, **A366**, 575–97 (1979).

[16]H. H. K. Xu and S. Jahanmir, "Microfracture and Material Removal in Scratching of Alumina," *J. Mater. Sci.*, **30**, 2235–47 (1995).

[17]Y.-G. Jung, I. M. Peterson, D. K. Kim, and B. R. Lawn, "Lifetime-Limiting Strength Degradation from Contact Fatigue in Dental Ceramics," *J. Dent. Res.*, **76** [2] 722–31 (2000).

[18]N. Axen, L. Kahlman, and I. M. Hutchings, "Correlations between Tangential Force and Damage Mechanisms in the Scratch Testing of Ceramics," *Tribol. Int.*, **30** [7] 467–74 (1997).

[19]F. Guiberteau, N. P. Padture, H. Cai, and B. R. Lawn, "Indentation Fatigue: A Simple Cyclic Hertzian Test for Measuring Damage Accumulation in Polycrystalline Ceramics," *Philos. Mag. A*, **68** [5] 1003–16 (1993).

[20]H. H. K. Xu and S. Jahanmir, "Scratching and Grinding of a Machinable Glass-Ceramic with Weak Interfaces and Rising *T*-Curve," *J. Am. Ceram. Soc.*, **78** [2] 497–500 (1995).

[21]F. Guiberteau, N. P. Padture, and B. R. Lawn, "Effect of Grain Size on Hertzian Contact in Alumina," *J. Am. Ceram. Soc.*, **77** [7] 1825–31 (1994).

[22]S. K. Lee, S. Wuttiphan, and B. R. Lawn, "Role of Microstructure in Hertzian Contact Damage in Silicon Nitride: I, Mechanical Characterization," *J. Am. Ceram. Soc.*, **80** [9] 2367–81 (1997).

[23]M. J. Readey, C. L. McCallen, P. McNamara, and B. R. Lawn, "Correlations Between Flaw Tolerance and Reliability in Zirconia," *J. Mater. Sci.*, **28** [24] 6748–52 (1993).

[24]S.-J. Cho, H. Moon, B. J. Hockey, and S. M. Hsu, "The Transition from Mild to Severe Wear in Alumina During Sliding," *Acta Metall.*, **40** [1] 185–92 (1992).

[25]C. He, Y. S. Wang, J. S. Wallace, and S. M. Hsu, "Effect of Microstructure on the Wear Transition of Zirconia-Toughned Alumina," *Wear*, **162–164**, 314–21 (1993).

[26]A. Pajares, L. Wei, B. R. Lawn, and D. B. Marshall, "Damage Accumulation and Cyclic Fatigue in Mg-PSZ at Hertzian Contacts," *J. Mater. Res.*, **10** [10] 2613–25 (1995). □